RAPID COMMUNICATIONS

PHYSICAL REVIEW C VOLUME 35, NUMBER 3 MARCH 1987

Line-shape analysis of high spin states: Collectivity in ^{166}Yb

J. C. Bacelar, R. M. Diamond, E. M. Beck, M. A. Deleplanque, J. Draper,* and F. S. Stephens
Nuclear Science Division, Lawrence Berkeley Laboratory, University of California, Berkeley, California, 94720
(Received 3 November 1986)

The Doppler-shift attenuation method was used to measure lifetimes of yrast states in ^{166}Yb. Three different stopping materials were used and consistent results were obtained over a large range of spins. Values of τ range from 1.20(10) ps at 18^+ to 0.05(1) ps at 34^+. The $B(E2)$ values steadily decrease from 200 to 120 single particle units as the spin increases above $24\hbar$. This loss of collectivity is likely to reflect a change toward triaxial shapes. The side-feeding times to these states are longer than the inband feeding times.

Nuclear structure at high spins has acquired a large body of data by means of gamma-ray spectroscopy[1-5] due primarily to the steady increase in experimental groups having at their disposal large arrays of high resolution Ge gamma-ray detectors. Such studies have initially concentrated on transition energies and spins. More recently, interest has focused on other quantities which can give us further insight into the nuclear structure. For example, the collectivity of nuclei at high spins, studied through the lifetime of the states, has been investigated by the Doppler shift attenuation method (DSAM) centroid, line-shape,[6] and recoil distance method (RDM)[7-9] techniques.

The DSAM techniques allow very fast transitions to be measured, $\sim$1 to $\sim$0.01 ps, whereas RDM can span the region from $\sim$1 ns up to a few tenths of a picosecond. There are difficulties in using DSAM methods, since in rotational bands fast transitions are associated with relatively high spins and therefore involve discrete line intensities which are typically less than 10% of a reaction channel. Large Doppler broadening and shifts create further difficulties in the analyses of these complex spectra, since not only do the peak to background ratios decrease, but also the broadened lines may overlap each other. In order to obtain clean enough spectra to measure the centroid or fit the line shape of such weakly populated transitions, one has to use coincidence techniques, for which the requirement of high statistics is imperative. This paper reports on the DSAM analyses of states in the yrast sequence of ^{166}Yb. Three different backings (stopping materials) were used, and therefore lifetime measurements on the same transitions were performed in well separated and different regions of the slowing-down process. The measurements span a large range of spins and almost overlap the RDM measurements previously performed in this nucleus.

The reaction used was 180 MeV ^{40}Ar+^{130}Te. The ^{40}Ar beam was provided by the Lawrence Berkeley Laboratory 88-inch cyclotron and four experiments were performed. For one experiment two thin Te targets (360 and 200 μg/cm^2) were stacked together and 90 million triple or higher gamma coincidence events were recorded on tape. In the other three experiments a 1 mg/cm^2 Te target on a $\sim$13 mg/cm^2 Au foil, Pb foil, and Mg foil were used, and 210, 150, and 11 million triple- or higher-fold-coincidence events were recorded, respectively. From the unbacked data the yrast sequence was extended from the previously published[10] data (24^+) up to the 38^+ level.[11] The 21 detectors of HERA subtended eight different angles to the beam direction ranging from 0° to 154°.[12] With the thin targets, the ^{166}Yb nuclei emitted gamma rays at the full recoil velocity, producing a peak at a different energy for each gamma ray at each detector angle. For the gamma rays that are emitted during the slowing-down process in the thick gold, lead or magnesium backings, deviations from the unbacked spectra were easily observed as Doppler broadened and shifted peaks.

To study in detail the lifetimes involved in the transitions observed, a Doppler-shift attenuation program was developed.[13] The production of ^{166}Yb nuclei was considered to be uniform throughout the target, with the initial recoiling velocity depending on the production position in the target. In the slowing-down process both electronic and nuclear stopping were considered. For the electronic stopping power, the tabulated values of Ref. 14 were used, corrected for the atomic shell structure of the stopping material.[15] For the nuclear stopping power, a multiple Coulomb scattering formalism was used,[16] with the magnitude and direction of the velocity for the recoiling ions in the target and backing materials calculated in a Monte Carlo fashion. The cross section for the nuclear Coulomb scattering increases as the velocity of the recoiling ions decreases; therefore this process is mostly important at low recoil velocities. Also at these lower velocities large-angle scattering occurs more and more frequently, imparting both large directional changes and large energy changes. This part of the slowing down process cannot easily be measured experimentally. Although the energy loss is obtainable, it is difficult to determine experimentally (model independently) the distance traveled in this regime. In our program, histories of velocities and directions versus time were stored, and profiles at each time step were averaged over typically 10000 histories for each of the stopping materials considered. The model used for the gamma-ray cascade decay has a rotational band with the known yrast discrete-line energies and a set of six rotational transitions with the same moment of inertia preceding the highest known transition. Lifetimes above spin 36 were chosen to give the best fit to the line shape of this transition ($36^+ \rightarrow 34^+$) observed in the Au-backed data. The subsequent decay was then allowed to proceed with individual lifetimes as free parameters. The side-feeding intensities

to these states (obtained experimentally from the unbacked data) were considered to come from rotational bands with the same transition energies as the yrast sequence. These bands were controlled by a single Q_0 moment which was a parameter in the fit, and for each state a new sideband with its own Q_0 was allowed. In this way the yrast-band lifetimes and the sideband feeding times were fitted at each spin. The data were then fitted for the forward, backward, and near 90° detector groups in the experimental setup. These three groups involved fourteen independent angles. The data were fitted for the three different backings. Since the target thicknesses were approximately the same with all three backings, the production of each yrast spin state was the same in each experiment, with the same feeding times. Therefore, as explained above, a certain transition gamma ray will occur at different stages of the slowing-down process for the different stopping materials, giving totally different line shapes (see Fig. 1). The 738.5-keV ($24^+ \rightarrow 22^+$) transition is emitted with a depopulation time profile which, while slowing down in Mg, senses a much faster recoiling velocity than in either of the other two stopping materials. This implies that in Mg, the line shape for this state (and all other states above it) is mainly sensitive to electronic stopping, whereas in Pb the line shape of the same state starts to be influenced by nuclear stopping, and in gold the line shape is caused mainly by the latter. Conversely, similar line shapes were obtained for different transition gamma rays (see Fig. 2) in different backings. With the Au backing, the 738.5-keV transition depopulating the 24^+ state has approximately the same line shape as the 580-keV transition depopulating the 20^+ state with the Pb-backed target, and as the 508-keV line depopulating the 18^+ state with the Mg-backed target. This means that a similar recoil velocity profile was obtained in Au at

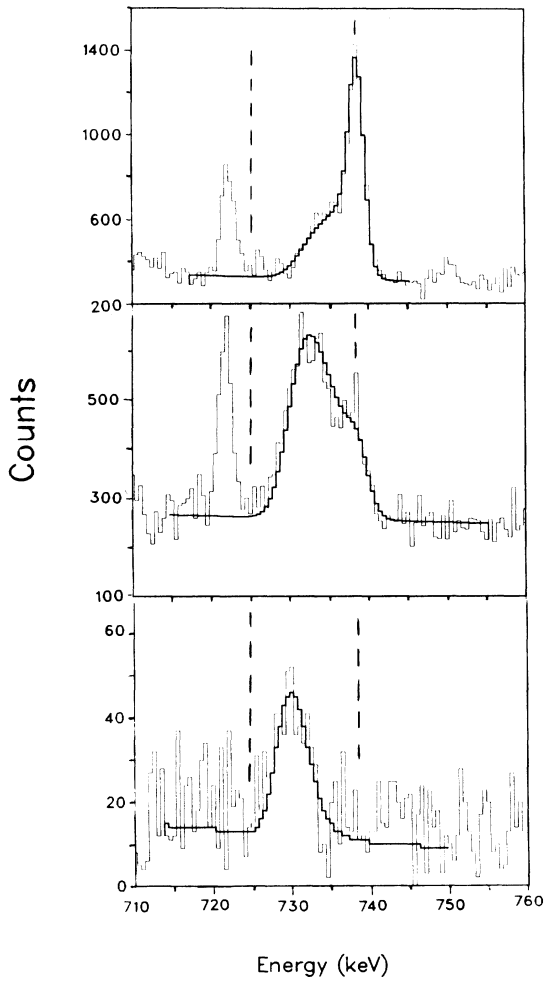

FIG. 1. Fits (thick line) to the 738.5-keV, $24^+ \rightarrow 22^+$ transition line shape, as observed by backward angle detectors (polar angle ~150° to the beam direction); Au backing (top), Pb backing (middle), and Mg backing (bottom). The left and right dashed vertical lines show the position of the fully shifted and stopped peaks, respectively. These spectra are gated by yrast transitions from 10^+ through 16^+, background subtracted. The sharp peak at 722.1 keV is the $14^+ \rightarrow 12^+$ cross-band transition and it shows poorly in the Mg-backed data due to statistics.

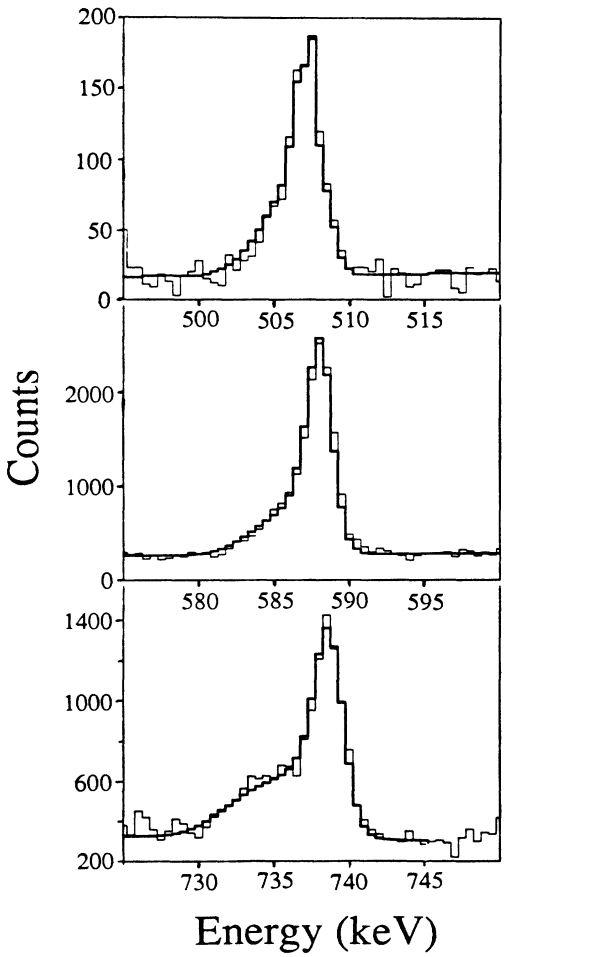

FIG. 2. Fits (thick line) to peaks observed at backward angles; 738.5-keV line ($24^+ \rightarrow 22^+$ transition) in Au-backed data (bottom), 588.5-keV line ($20^+ \rightarrow 18^+$ transition) in Pb-backed data (middle), and 508.2-keV line ($18^+ \rightarrow 16^+$ transition) in Mg-backed data (top). (See also caption of Fig. 1.)

TABLE I. Lifetimes in ^{166}Yb.

I_i	Int.[a]	E_γ (keV)	τ(ps) Au	τ(ps) Pb	τ(ps) Mg	τ(ps)[b]	$B_w(E2)$[c] Single particle units
18	48.0	508.1			1.18(15)	1.18(15)	208(30)
20	31.0	588.0		0.57(6)	0.59(5)	0.59(5)	208(18)
22	22.0	666.2		0.26(3)	0.30(3)	0.29(3)	218(22)
24	16.2	738.9	0.16(2)	0.18(2)	0.18(2)	0.18(2)	212(22)
26	12.0	806.0	0.10(1)	0.12(1)	0.12(1)	0.12(1)	204(20)
28	7.8	870.2	0.10(1)	0.10(1)		0.10(1)	166(18)
30	6.4	935.0	0.08(1)	0.08(1)		0.08(1)	144(18)
32	3.7	1000.5	0.06(1)	0.06(1)		0.06(1)	138(22)
34	2.9	1060.0	0.05(1)			0.05(1)	123(25)

[a]Intensities of the transitions in percent relative to the 4^+ decay.
[b]These lifetimes are average lifetimes weighted toward the slowest material (75% weight factor).
[c]$B_w(E2)^{-1} = \frac{1}{5}\langle I_i | I_f\rangle^2 \tau E_\gamma^5$; E_γ(MeV), τ(ps), and the Clebsch-Gordon coefficient $\langle I_i | I_f\rangle^2 \sim 0.36$ for this region of spin. The lifetimes used are from column 7.

the time of emission of the $24^+ \rightarrow 22^+$ transition as in the later emission time of the $20^+ \rightarrow 18^+$ transition in Pb backing, and even later for the $18^+ \rightarrow 16^+$ transition in Mg. The fits obtained at backward angles for some transitions are given in Figs. 1 and 2. Table I contains a summary of the results. The relative errors in the lifetime and feeding times obtained in such fits are small since the number of data points exceeds the number of free parameters, particularly since three different detector groups are fitted simultaneously. Therefore, we believe that the largest source of uncertainty (not reflected in the error bars of Fig. 3 and Table I) comes from systematic errors in the treatment of the slowing-down process. However, the lifetimes of the fastest transitions in the Pb backing are consistent with the same transitions in the Au backing. The only time that the feeding time to a state was "mocked up" by unobserved preceding transitions was for the 36^+ state in Au. The same feeding time and subsequent lifetimes determined with the Au backing were then used and gave a good fit for the $32^+ \rightarrow 30^+$ transition in the Pb backing, which was the highest transition fitted in that backing. These observations indicate that the electronic slowing down is well treated in the analyses for these two, quite different materials. Also for the gamma ray depopulating the 26^+ state (the highest fitted with the Mg-backed target), the same feeding time and lifetime were obtained for Mg as for Pb backings. On the other hand, the lower transitions in Au, $26^+ \rightarrow 24^+$ and $24^+ \rightarrow 22^+$, show faster lifetimes than the results for Pb backing (see Table I). The same effect is noted for the lowest transition measured with the Pb-backed target as compared to the Mg-backed one. This might be evidence that both in Au and Pb the effects of nuclear stopping were overestimated. Nevertheless, none of the lifetimes measured with the different backings differ more than 20%, with a surprisingly good agreement for the fastest transitions; the only systematic discrepancies occurred near the stopped line shapes. These results also agree with the highest measured lifetimes from the RDM technique.

Both lifetimes and derived $B(E2)$ values are given in Table I. As described in the previous work[6] containing only Au-backed data, there is a loss of collectivity toward higher spins but, even at 34^+ the nucleus remains very collective [123 single particle units (spu)]. The decrease in $B(E2)$ values can result from a decreasing quadrupole deformation or an increasing triaxiality ($\gamma \neq 0$), as can be seen from the relation[18] $B(E2) \approx \beta^2 \cos^2(30+\gamma)$. Limits can be obtained with this simple formula for the shape changes associated with the drop in $B(E2)$ to 123 spu. If it is only an elongation change ($\gamma = 0$), then β drops to

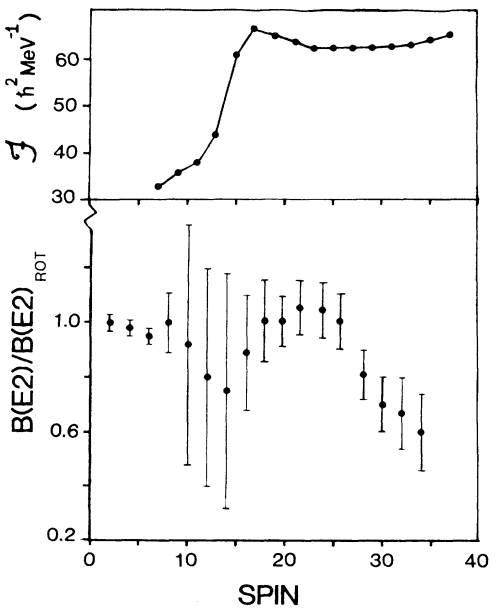

FIG. 3. Variations of $B(E2)/B(E2)_{rotor}$ and the kinetic moment of inertia (J) vs spin, are shown for ^{166}Yb yrast states. The low spin ($< 18^+$) $B(E2)$ data are from Ref. 17. The moment of inertia is taken from measured transition energies, Ref. 11. The $B(E2)/B(E2)_{rotor}$ values are normalized to 1.0 for the $2^+ \rightarrow 0^+$ transition.

0.24, instead of the ground state value of 0.3. However, for a well deformed nucleus like ^{166}Yb, the potential is calculated[19] to be rather stiff for changes on β. If the change is solely in γ (for $\beta=0.3$), it is then consistent with γ increasing from 0° to ~15°. These variations are only limits for the shape parameters, since a combination of changes in the quadrupole deformation and γ is possible. It should be mentioned that the sidebands which feed the yrast states have longer feeding times, showing either less collectivity [$B(E2)$ values ~60 spu], or larger moments of inertia (~25% larger).

Angular momentum alignments, i.e., occupation or depopulation of specific particle orbitals, can induce shape changes of the equilibrium deformation of the mean field.[20] However, a second alignment in ^{166}Yb is not apparent in the gamma-ray energies in the spin region where the $B(E2)$ values decrease. If present it should cause an increase in the moment of inertia J, whereas J is rather constant in Fig. 3. It may also be noted that in the region of constant $B(E2)$'s (spin 0–10$\hbar$ and 18–24$\hbar$), J changes. But J is sensitive to a number of properties, e.g., alignments, the nuclear shape, and the pairing correlations, whereas the $B(E2)$ values are sensitive essentially only to the shape. The increase in J in the lower spin regions is reflecting the gain in alignment and loss of pairing associated with breaking the first paired neutron state ($i_{13/2}$ orbital). The large and constant $B(E2)$ values measured above this alignment (spins 18–24$\hbar$) reflect the rigidity of the potential to shape changes. This is in contrast with the softer nuclei at the beginning of the $i_{13/2}$ shell $N\sim90$, where the first alignment produces a drastic drop in the $B(E2)$ values.[7–9] For the highest spin region (above spin 24$\hbar$), if the shape is changing, as indicated by the loss of collectivity, an equivalent drop in the moment of inertia would be expected. But the alignment of the particles inducing such shape changes and the consequent drop in the pairing energy both would tend to increase the moment of inertia, essentially canceling the effect of the shape change. While it would not be surprising to find alignments, shape changes, and pairing changes systematically interrelated in this region, still the nearly constant values of J in so many cases[4] suggest that a more general explanation may be involved.

In summary, line shape analyses of transitions in coincidence with high-spin discrete-line gates were used to extract lifetimes of high-spin states in the yrast sequence of ^{166}Yb. By using three different stopping materials we determined the lifetimes from levels 18^+ through 34^+. The three different materials gave results that were consistent to 20%. We find that the yrast states in ^{166}Yb start losing collectivity only above spin 26$\hbar$. This may be interpreted as a movement toward triaxial deformation of the equilibrium nuclear shape at these spins, whereas the shape of this nucleus appears quite stable at lower spins, in contrast to the lighter Yb isotopes.

This work was supported by the U.S. Department of Energy under Contract No. DE-AC03-76SF00098.

*Permanent address: University of California, Davis, CA 95616.

[1]J. C. Bacelar, M. Diebel, C. Ellegaard, J. D. Garrett, G. B. Hagemann, B. Herskind, A. Holm, C.-X. Yang, J.-Y. Zhang, P. O. Tjøm, and J. C. Lisle, Nucl. Phys. **A442**, 509 (1985), and references therein.

[2]B. Haas, D. Ward, H. R. Andrews, O. Hausser, A. J. Ferguson, J. F. Sharpey-Schafer, T. K. Alexander, W. Trautmann, D. Horn, P. Taras, P. Skensved, T. L. Khoo, R. K. Smither, I. Ahmad, C. N. Davids, W. Kutschera, S. Levenson, and C. L. Doors, Nucl. Phys. **A362**, 254 (1981).

[3]F. S. Stephens, M. A. Deleplanque, R. M. Diamond, A. O. Macchiavelli, and J. E. Draper, Phys. Rev. Lett. **54**, 25 (1985).

[4]R. Chapman, J. C. Lisle, J. N. Mo, E. Paul, A. Simcock, J. C. Willmott, J. R. Leslie, H. G. Price, P. M. Walker, J. C. Bacelar, J. D. Garrett, G. B. Hagemann, B. Herskind, A. Holm, and P. J. Nolan, Phys. Rev. Lett. **51**, 2265 (1983).

[5]P. J. Twin, B. M. Nyako, A. H. Nelson, J. Simpson, M. A. Bentley, H. W. Cranmer-Gordon, P. D. Forsyth, D. Howe, A. R. Mokhtar, J. D. Morrison, J. F. Sharpey-Schafer, and G. Sletten, Phys. Rev. Lett. **57**, 811 (1986).

[6]J. C. Bacelar, A. Holm, R. M. Diamond, E. M. Beck, M. A. Deleplanque, J. Draper, B. Herskind, and F. S. Stephens, Phys. Rev. Lett. **57**, 3019 (1986).

[7]A. Pakkanen, Y. H. Chung, P. J. Daly, S. R. Faber, H. Helppi, J. Wilson, P. Chowdhury, T. L. Khoo, I. Ahmad, J. Borggreen, Z. W. Grabowski, and D. C. Radford, Phys. Rev. Lett. **48**, 1530 (1982).

[8]H. Emling, E. Grosse, R. Kulessa, D. Schwalm, R. S. Simon, D. Husar, H. J. Wollersheim, and D. Pelte, Phys. Lett. **98B**, 169 (1981).

[9]M. P. Fewell, N. R. Johnson, F. K. McGowan, J. S. Hattula, I. Y. Lee, C. Baktash, Y. Schutz, J. C. Wells, L. L. Riedinger, M. W. Guidry, and S. C. Pancholi, Phys. Rev. C **31**, 1057 (1985).

[10]W. Walus, N. Roy, S. Jonsson, L. Carlen, H. Ryde, G. B. Hagemann, B. Herskind, J. D. Garrett, Y. S. Chen, J. Almberger, and G. Leander, Phys. Scr. **24**, 324 (1981).

[11]E. M. Beck, J. C. Bacelar, M. A. Deleplanque, R. M. Diamond, F. S. Stephens, J. Draper, B. Herskind, A. Holm, and P. O. Tjøm, Nucl Phys. (to be published).

[12]R. M. Diamond and F. S. Stephens (unpublished); R. M. Diamond, in *Instrumentation for Heavy-Ion Nuclear Research,* edited by D. Shapira (Harwood, New York, 1985), p. 259.

[13]J. C. Bacelar, Nucl. Instrum. Methods Phys. Res. (to be published).

[14]L. C. Northcliffe and R. F. Schilling, Nucl. Data Tables **7**, 233 (1970).

[15]J. F. Ziegler and W. K. Chu, Nucl. Data Tables **13**, 463 (1974).

[16]J. Lindhard, M. Scharff, and H. E. Schiott, K. Dan. Vidensk. Selsk. Mat. Fys. Medd. **33**, 14 (1963).

[17]B. Bochev, S. A. Karamian, T. Kutsarova, E. Nadjakov, and Yu. Ts. Oganessian, Nucl. Phys. **A267**, 344 (1976).

[18]A. Bohr and B. Mottelson, *Nuclear Structure* (Benjamin, Reading, MA, 1975), Vol. II, p. 164.

[19]J-Y. Zhang and S. Aberg, Nucl. Phys. **A390**, 314 (1982).

[20]Y. S. Chen, S. Frauendorf, and L. L. Riedinger, Phys. Lett. **171B**, 7 (1986).